

Encapsulation of Small Gas Molecules by Cryptophane-111 in Organic Solution. 1. Size- and Shape-Selective Complexation of Simple Hydrocarbons

Kathleen E. Chaffee,^{‡,§} Heather A. Fogarty,[†] Thierry Brotin,^{†,*} Boyd M. Goodson,[‡] and Jean-Pierre Dutasta^{†,*}

Laboratoire de Chimie, CNRS, École Normale Supérieure de Lyon, 46 Allée d'Italie, F-69364 Lyon 07, France and the Department of Chemistry and Biochemistry, 113 Neckers Building, Southern Illinois University, Carbondale, Illinois 62901, United States of America

Received: April 15, 2009; Revised Manuscript Received: September 6, 2009

The reversible trapping of small hydrocarbons and other gases by cryptophane-111 (**1**) in organic solution was characterized with variable-temperature ¹H NMR spectroscopy. Characteristic spectral changes observed upon guest binding allowed kinetic and thermodynamic data to be readily extracted, permitting quantification and comparison of different host–guest interactions. Previous work (*J. Am. Chem. Soc.* **2007**, 129, 10332) demonstrated that **1**, the smallest cryptophane to date, forms a complex with xenon with remarkably high affinity. Presently, it is shown that **1** also exhibits slow exchange dynamics with methane at reduced temperatures ($\delta_{\text{bound}} = -5.2$ ppm) with an association constant $K_a = 148 \text{ M}^{-1}$ at 298 K. In contrast, ethane and ethylene are poorly recognized by **1** with K_a values of only 2 M^{-1} and 22 M^{-1} , respectively; moreover, chloromethane (whose molecular volume is similar to that of xenon, $\sim 42 \text{ \AA}^3$) is not observed to bind to **1**. Separately, molecular hydrogen (H_2) gas is observed to bind **1**, but in contrast to other ligands presently studied, H_2 complexation is spectrally manifested by fast exchange throughout virtually the entire range of available conditions, as well as by a complex dependence of the guest ¹H resonance frequency upon temperature and host concentration. Taken together, these results establish **1** as a selective host for small gases, with implications for the design of size- and geometry-selective sensors targeted for various gas molecules.

1. Introduction

Over the last two decades there has been increasing interest in supramolecular systems capable of encapsulating small neutral molecules,^{1–6} spurred in part by the desire to tune the characteristics of host cavities (including size, shape, polarity, and chirality⁷) to achieve greater guest selectivity. For example, considerable work has investigated the design and binding properties of supramolecular receptors and hydrogen-bonded dimeric capsules.⁸ Such dimeric receptors typically have relatively large internal cavities that exhibit specific molecular recognition for correspondingly sized molecules, and are often able to encapsulate more than one substrate in organic and aqueous solutions (thus permitting, for example, chemical reactions to take place inside those cavities).^{9–11}

However, host molecules or materials specifically designed to recognize *smaller* molecules may also find application in many fields, such as environmental chemistry,¹² chemical storage,¹³ sensors,¹⁴ and chemical separations;¹⁵ moreover, fundamental studies of inclusion complexes involving small, prototypical guests may provide new insight into how such molecules interact with their surrounding environment. However, relatively few systems capable of molecular recognition of small gaseous substrates (e.g., hydrogen, carbon dioxide, nitrogen oxides, or simple hydrocarbons) have been reported.^{3,16} For example, gases such as Cl_2 , Kr, Xe, O_2 , CO_2 , C_2H_4 , CH_4 , C_2H_6 , and $n\text{-C}_4\text{H}_{10}$ have been demonstrated to bind with

α -cyclodextrin in aqueous solutions.¹⁷ Additionally, hemicerands (covalently sealed molecular containers) have been shown to encapsulate O_2 , N_2 , CO_2 , and Xe in organic solutions,¹⁸ and Rebek and co-workers have demonstrated that hydrogen-bonded dimeric capsules could encapsulate gases such as CH_4 , C_2H_4 , cyclopropane, and Xe in CDCl_3 solvent.^{19,20} In the 1990s, Collet and co-workers reported the synthesis of cryptophane molecules that demonstrate strong affinities for a number of small hydrocarbons, including the encapsulation of methane by cryptophane-A in organic solution;^{16,21–24} later, cryptophanes were demonstrated to encapsulate Xe as well.^{25–29} Furthermore, Naruta and co-workers reported the synthesis of a cavitand-porphyrin capsule showing high affinity for methane in chloroform³⁰ and Fabris and co-workers described the synthesis of a chiral dimeric capsule possessing an extraordinarily small internal cavity (46 \AA^3) that exhibits strong affinities for methane and nitrogen.³¹ More recently, Gibb and co-workers described the synthesis of molecular capsules that exhibit very high affinities for butane (and to a lesser extent for propane) in water.⁸ Finally, it should be mentioned that a large number of solid-state materials have also been investigated for gas storage and separations (e.g., ref 32); however, in such materials the gases are often partitioned into large lattice voids or interstitial spaces, and the nature of the molecular recognition may be quite different from the solution-state encapsulation of interest here.

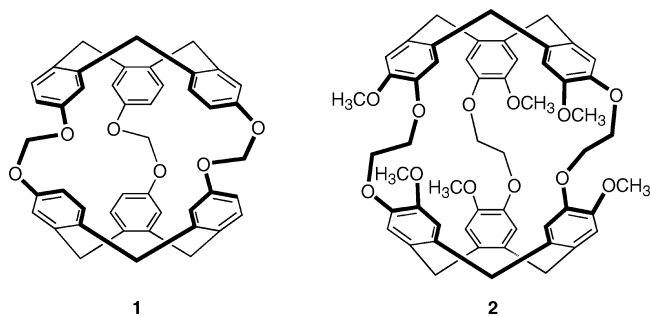
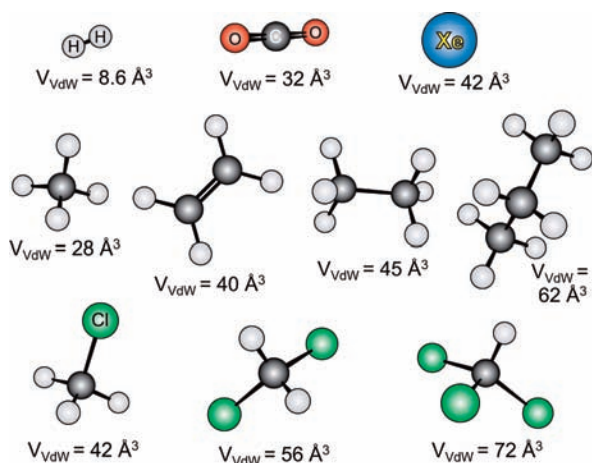
The design of ideal host systems for small gas molecules is hampered by the weakness of available host–guest interactions. Nevertheless, correspondingly small lipophilic cavities appear to be key attributes for the efficient encapsulation of such guests. Being hollow polyarene compounds, cryptophanes (e.g., Chart 1) provide such lipophilic cavities suitable for encapsulation of small neutral molecules;²⁵ moreover, the volume and acces-

* To whom correspondence should be addressed. E-mail: Thierry.Brotin@ens-lyon.fr; Jean-Pierre.Dutasta@ens-lyon.fr.

[†] École Normale Supérieure de Lyon.

[‡] Southern Illinois University, Carbondale.

[§] Current address: Department of Radiology, Washington University School of Medicine, St. Louis, MO 63110, USA.

CHART 1: Structure of Cryptophane-111 (1) and Cryptophane-A (2)**CHART 2: Guest Molecules with Corresponding van der Waals volume (V_{vdw}) Values**

sibility (and to some degree, the geometry and flexibility) of these cavities may be systematically varied by choosing differently sized linker moieties and capping groups.

For example, cryptophane-A (2) demonstrates a binding preference for relatively small, roughly tetrahedral molecules such as dichloromethane (CH_2Cl_2) and chloroform (CHCl_3), as well as strong affinities for the smaller (and more symmetrical) species methane and xenon—two substances able to interact only weakly with their surrounding environments via van der Waals interactions. In comparison, cryptophanes that possess larger internal cavities (e.g., cryptophane-E, not shown) can bind larger guests.³³ Conversely, cryptophane-111 (1), the smallest cryptophane to date possessing a rigid cavity of only $\sim 81 \text{ \AA}^3$, was recently shown to exhibit remarkable binding behavior with xenon in organic solutions, including an exceptionally strong association constant ($K_a = 10^4 \text{ M}^{-1}$ at 298 K).³⁴ Given such striking binding properties and the corresponding insight that might be gained for potential applications, the binding behavior of 1 and a variety of other small gas species is thus of immediate interest.

Here we report the investigation of the reversible trapping of simple hydrocarbons and other small gases (Chart 2) by 1 in organic solution using ^1H variable-temperature NMR spectroscopy. Ligand binding is manifested by characteristic changes in both host and guest NMR signals, allowing both kinetic and thermodynamic data to be readily extracted from the (“bound” and “free”) guest resonances to permit quantification and comparison of different host–guest interactions. For example, 1 is observed to exhibit slow exchange dynamics with methane at reduced temperatures ($\delta_{\text{bound}} = -5.2 \text{ ppm}$) with an association constant of $K_a = 262 \text{ M}^{-1}$ at 245 K, extrapolating to 148 M^{-1}

at 298 K. In contrast, ethane and ethylene are poorly recognized by 1 with extrapolated room-temperature K_a values of 2 M^{-1} and 22 M^{-1} , respectively; moreover, complexation of 1 with propane and larger gases was not observed. Similarly, 1 also failed to exhibit binding with chloromethane, despite its nearly identical volume to that of xenon ($\sim 42 \text{ \AA}^3$). Separately, molecular hydrogen (H_2) gas is observed to bind 1, but (in contrast to other ligands presently studied) the apparent complexation is manifested by fast exchange throughout the entire range of available conditions, as well as an unexpected ^1H chemical shift dependence upon temperature and host concentration that is not consistent with a 1:1 host:guest ratio (results to be reported in greater detail in part 2 of this contribution).³⁵ Taken together, these results establish 1 as a selective host for small gases, with implications for the design of size- and geometry-selective hosts for separation or sensing applications.

2. Methods

The NMR spectra of the complexes between 1 and various ligands are analyzed in terms of conventional host–guest equilibria. Unless stated otherwise, for each guest a 1:1 complex is assumed to form at equilibrium with 1 according to the relation:



where k_1 and k_{-1} are the rates of complexation and decomplexation, respectively. The association equilibrium constant (K_a) at a given temperature may be readily extracted using the following:

$$K_a = \frac{k_1}{k_{-1}} = \frac{[\text{HG}]}{[\text{H}][\text{G}]} = \frac{[\text{HG}]}{(c(\text{H}) - [\text{HG}]) (c(\text{G}) - [\text{HG}])} \quad (2)$$

where $[\text{H}]$, $[\text{G}]$, and $[\text{HG}]$ are respectively the equilibrium concentrations of the host, guest, and complex, and $c(\text{H})$ and $c(\text{G})$ are respectively the initial concentrations of the host and guest molecules. Thus, provided that the guest exchange is slow with respect to the NMR time scale (i.e., where: k_{-1} is sufficiently less than $|\nu_f - \nu_b|$, the difference between the intrinsic resonance frequencies of the free and bound guests), K_a values can be determined by integration of the bound guest, free guest, and selected host resonances (and knowledge of the initial host concentration). Additionally, kinetic parameters can be estimated from the linewidths of the bound guest resonances according to $k_{-1} = \pi \Delta \nu_{\text{fwhm}}$ (i.e., the full width at half-maximum of the bound guest peak), assuming that the guest line width is dominated by exchange broadening.

Measurements taken from ^1H NMR spectra obtained at different temperatures may be combined to determine various thermodynamic parameters that govern a given host–guest interaction. For example, temperature-dependent K_a values may be plotted according to the van't Hoff equation:

$$\ln(K_a) = -\frac{\Delta H^\circ}{RT} + \frac{\Delta S^\circ}{R} \quad (3)$$

where T is the temperature in Kelvin, R is the ideal gas constant ($8.314 \text{ J K}^{-1} \text{ mol}^{-1}$), and ΔH° and ΔS° are the enthalpy and the entropy of formation, respectively (giving the Gibb's free

TABLE 1: van der Waals Volumes of Guest, ^1H NMR Chemical Shifts ($\Delta\delta = \delta_t - \delta_b$), Binding Constants (K_a), Free Energies of Association (ΔG°), Enthalpies of Association (ΔH°), Entropies of Association (ΔS°), Energy Barriers for Dissociation (ΔG^\ddagger), Enthalpy Barriers for Dissociation, And the Activation Energies (E_a) for Some Complexes of Cryptophane-111 (**1**) in CDCl_3 and Cryptophane-A (**2**) in $\text{C}_2\text{D}_2\text{Cl}_4$ with Various Guests

guest	host	V_{vdw} (\AA^3)	δ (ppm)	K_a (M^{-1}) (298 K)	ΔG° (kJ mol^{-1})	ΔH° (kJ mol^{-1})	ΔS° ($\text{Jmol}^{-1} \text{K}^{-1}$)	ΔG^\ddagger (kJ mol^{-1})	ΔH^\ddagger (kJ mol^{-1})	ΔS^\ddagger ($\text{Jmol}^{-1} \text{K}^{-1}$)	E_a (kJ mol^{-1})
Xe^{34}	1	42	+ 30 ^c	10^4	-22.8			64.9 ± 3	43.2 ± 1.6	-74.0 ± 3	
CH_4	1	28	- 5.3	148.0	-12	-9.9 ± 0.7^a	5.9 ± 3.1^a	49.7 ± 2.8^a	41.1 ± 1.2^a	-28.6 ± 5^a	43.1 ± 1.1^a
						-7.4 ± 0.3^b	16.8 ± 3.2^b	52 ± 4^b	34.4 ± 2^b	-58 ± 8^b	36.2 ± 1.1^b
C_2H_4	1	40	- 5.0	22.5	-7.7	-9.3 ± 1.3	-5.4 ± 6.1	45.4 ± 0.8	36.4 ± 0.8	-30.8 ± 4	38.2 ± 0.8
C_2H_6	1	45	- 4.8	2.4	-2.2	-6.5 ± 0.6	-14.7 ± 2.9	46.4 ± 0.8	36.9 ± 0.7	-31.8 ± 3	38.7 ± 0.7
$\text{Xe}^{29,34,65}$	2	42	+ 62.3 ^c	3900^d	-19.1			53.4	35.5 ± 2	-60.0 ± 5	37.5
CH_4	2	28	- 4.5	130 ± 20	-11.3	-6.7	17.0	44.0			
CH_4	2	28	-4.5	90	-11.1						
CH_3Cl	1	42	does not bind								
C_3H_8	1	62	does not bind								
CHCl_3	1	72	does not bind								
CH_2Cl_2	1	56	does not bind								

^aData given for the high temperature fit. ^bData given for the overall fit. ^cReference given with respect to xenon gas extrapolated to zero pressure. ^dData given at 278 K.

energy $\Delta G^\circ = \Delta H^\circ - T \Delta S^\circ$). Next, values for k_{-1} can be plotted as dictated by conventional transition-state theory via the Eyring Equation:

$$\ln\left(\frac{k_{-1}}{T}\right) = -\frac{\Delta H^\ddagger}{R} \cdot \frac{1}{T} + \ln\left(\frac{k_B}{h}\right) + \left(\frac{\Delta S^\ddagger}{R}\right) \quad (4)$$

thereby permitting straightforward extraction of the enthalpy, ΔH^\ddagger , and the entropy, ΔS^\ddagger , of activation (and hence the free activation energy $\Delta G^\ddagger = \Delta H^\ddagger - T\Delta S^\ddagger$); here k_B and h are respectively Boltzmann's and Planck's constants. Similarly, the temperature-dependent rate of guest exchange can be related to the activation energy, E_a , for a given process according to the Arrhenius equation:

$$\ln(k_{-1}) = -\frac{E_a}{RT} + \ln(A) \quad (5)$$

where A is the pre-exponential factor. All of the results are discussed in Section 4 and the corresponding thermodynamic and kinetic data are summarized below in Table 1.

3. Experimental Section

Cryptophane-111 (**1**) and cryptophane-A (**2**) were synthesized according to procedures described in refs 36–38 For most samples, **1**/guest solutions were prepared using 0.5–0.9 mg of host dissolved in a known amount of CDCl_3 solvent (500–700 μL) to provide solutions with ~ 2 mM host concentration (note that the CDCl_3 solvent molecules are too large to fit within the cavity of **1**). Host solutions were loaded into a 5-mm stopcock-sealable NMR tube and a given (gas-phase) guest species was flowed into the sample tube for a few seconds, sealed, shaken, and allowed to equilibrate for at least 1 day. H_2 @**1** samples were prepared using different amounts of host (0.1–1.5 mg) dissolved in CDCl_3 (500 μL). The samples were degassed using the freeze–pump–thaw method and the evaluated samples were loaded with pure hydrogen gas from a balloon. K_a and k_{-1} values for a given guest/**1** complex were calculated from ^1H NMR spectra obtained with a Bruker spectrometer (operating at 500 MHz) and 5-mm liquids probe (nonspinning); variable temperature (VT) experiments were calibrated with methanol.

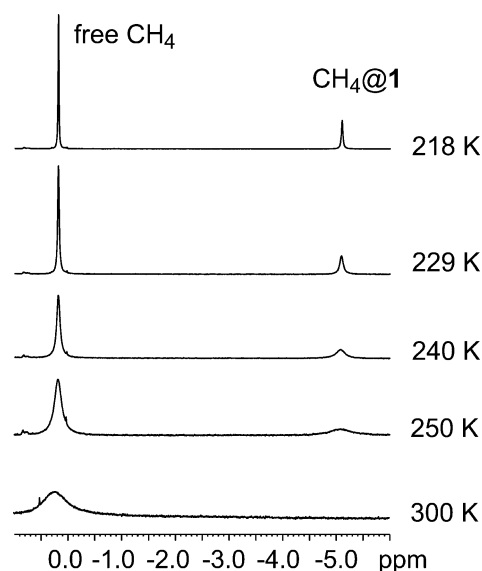


Figure 1. Upfield portions of selected ^1H VT NMR spectra showing the formation of the CH_4 @**1** complex.

Computational modeling of the host **1** and the complex C_2H_4 @**1** was performed with the CONFLEX method for generating low-energy conformers using Augmented MM3 parameters implemented within CAChe v.7.5.0.85.³⁹

4. Results and Discussion

Methane Complexation by Host 1 (and 2). The complexation of methane by **1** in chloroform solvent was investigated by VT ^1H NMR spectroscopy; relevant portions of selected spectra are shown in Figure 1. Upon loading with methane, a single (relatively broad) new peak located at ~ 0 ppm is observed at room temperature, assigned to free methane in solution. Following a reduction in temperature a second, much higher-field signal is readily apparent at ~ -5.10 ppm, indicating the formation of a CH_4 @**1** complex in the slow-exchange regime. For example, spectra obtained below ~ 260 K give rise to broad but distinct resonances for bound and free signals, with increasingly narrow lines at lower temperatures (as expected for reduced rates of chemical exchange for the guests). The large upfield chemical-shift difference observed between the free and bound guest NMR signals is characteristic of the shielding effect

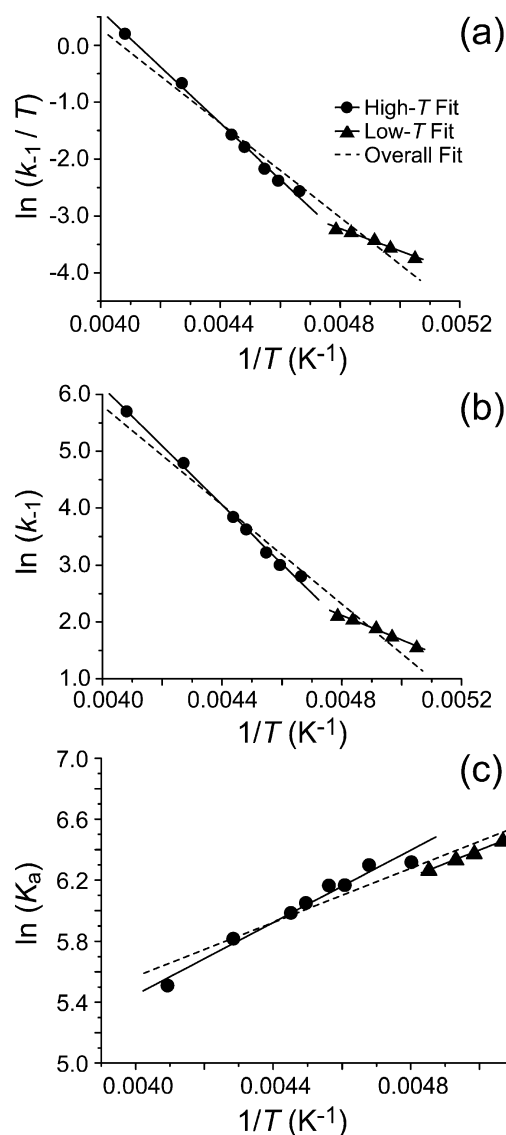


Figure 2. Eyring (a), Arrhenius (b), and van't Hoff (c) plots for the determination of kinetic and thermodynamic data for the complexation of CH_4 by **1**. The data in (a) and (b) have been corrected for the intrinsic line width estimated for each spectrum (no more than $\sim 1\text{--}2$ Hz).

induced by the host's six aromatic rings upon the nuclear spins of the trapped methane guest as it samples the interior cavity space of **1**.

The slow exchange dynamics observed over a wide range of temperatures allows the facile determination of both the thermodynamic and kinetic parameters governing the complex. Correspondingly, Eyring, Arrhenius, and van't Hoff plots (Figure 2) were constructed from data extracted from ^1H NMR spectra recorded as low as 197 K (near the freezing point of the solution; note that the freezing point of neat chloroform is 209 K). While overall, the data plotted in Figure 2 are consistent with the expected qualitative trends for host-guest binding, the data are not well-reproduced with a single linear fit; instead it appears that the decreases in $\ln(k_{-1}/T)$ in Figure 2(b) [and in $\ln(k_{-1})$, Figure 2(a)] as a function of $1/T$ can be decomposed into two different regimes: First a linear decrease going from 244 to 212.8 K is observed [high- T fit, Figure 2(b)], which is characterized by an activation energy $E_a = 43.1$ $\text{kJ}\cdot\text{mol}^{-1}$. At lower temperatures [low- T fit, Figure 2(b)] a second linear variation is characterized by a smaller value for the activation energy (18.0 $\text{kJ}\cdot\text{mol}^{-1}$); note that the apparent deviation from

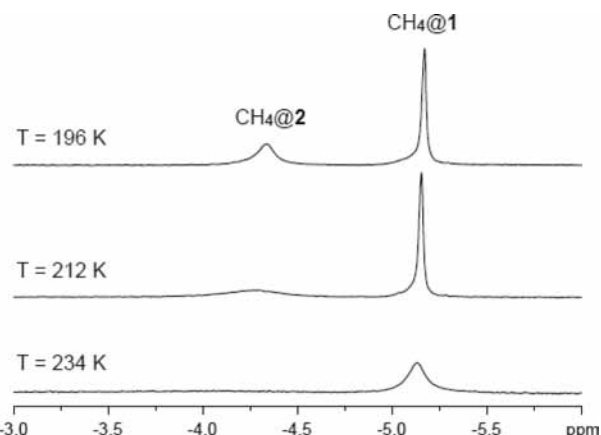


Figure 3. Portions of selected ^1H VT NMR spectra taken from a competition experiment between hosts **1** and **2** using methane as the guest (and a solvent comprised of 1,1,2,2-tetrachloroethane- d_2 and toluene- d_8); only the bound resonances from the guest are shown.

linearity in the data, while mild, is maintained even when the data are corrected for the (small) intrinsic line width (generally $<1\text{--}2$ Hz). Such bilinear behavior is also observed in the van't Hoff plot (Figure 2(c)), and could reflect a temperature-dependence of E_a (and/or ΔH°) for complexation/decomplexation. In any case, for more reliable comparison with the values obtained with other ligands, we have largely disregarded the low-temperature data and correspondingly used the kinetic and thermodynamic parameters derived from the high-temperature fits throughout the remainder of this work.

Although the $\text{CH}_4@1$ complex is not in slow exchange at room temperature, the higher-temperature data in the van't Hoff plot (Figure 2(c)) may be extrapolated with eqs 2 and 3 to give an estimated binding constant of $K_a = 148$ M^{-1} at 298 K. Somewhat surprisingly, this value is only slightly larger than that originally reported for the $\text{CH}_4@2$ complex ($K_a = 130$ M^{-1} at 298 K).¹⁶ Although the latter value was reported from a study using 1,1,2,2-tetrachloroethane- d_2 as the solvent (instead of the presently utilized deuterated chloroform), this small change in solvent type is not expected to have a significant effect on methane binding by **1**; thus, it would be somewhat unexpected that these methane/cryptophane K_a values should be so similar given the significantly smaller cavity size of **1** ($V_{\text{vdw}} = 81$ \AA^3) vs that of **2** ($V_{\text{vdw}} = 95$ \AA^3).

A competition experiment between the two hosts was performed to fairly compare the two cryptophane molecules for methane affinity. A solution containing **1** and **2** was prepared by dissolving equimolar amounts of both hosts (1 mM) in a mixture of 1,1,2,2-tetrachloroethane- d_2 and toluene; this solvent choice provides sufficient cryptophane solubility and allows study over the necessary temperature range while avoiding the use of smaller molecules (such as chloroform) that can bind within the larger cavity of **2**. Results from the competition experiment are summarized in Figure 3. For example, at 234 K only one broad resonance at -5.15 ppm was observed, characteristic of formation of the $\text{CH}_4@1$ complex under slow-exchange conditions. At lower temperatures (<215 K), however, the competition experiment revealed two distinct upfield-shifted signals located at -4.35 ppm and -5.15 ppm, respectively, corresponding to methane gas encapsulated in hosts **2** and **1** (Figure 3 top). At 196 K, both the linewidth and integration values of the two bound signals clearly indicate that the complex of methane with **1** is significantly stronger, and in slower exchange, than that with **2**; the 1.7-fold larger value for the integral of the $\text{CH}_4@1$ compared to $\text{CH}_4@2$ correspond to a

new K_a for the $\text{CH}_4@2$ complex of 466 M^{-1} at 196 K (compared to the corresponding value for $\text{CH}_4@1$ of 695 M^{-1} at 196 K). The ~ 1.7 -fold larger integral was fairly constant over the available temperature range, corresponding to an extrapolated K_a value for $\text{CH}_4@2$ of $\sim 90 \text{ M}^{-1}$ at 298 K. This new lower value was essentially confirmed by repeating the original single-cage complexation experiment (using only host **2** in presence of methane solution; results not shown) that gave an extrapolated K_a value for $\text{CH}_4@2$ of $\sim 80 \text{ M}^{-1}$ at 298 K, further supporting that the binding constant for the $\text{CH}_4@2$ complex reported in the original paper was overestimated.¹⁶

The kinetic and thermodynamic parameters governing the complexation of methane by **1** and **2** are summarized in Table 1. The stabilization of both $\text{CH}_4@1$ and $\text{CH}_4@2$ complexes is both enthalpic and entropic in origin, as indicated by negative Gibbs energy values (e.g., $\Delta G^\circ = -12.4 \text{ kJ}\cdot\text{mol}^{-1}$ at 298 K for $\text{CH}_4@1$). It is likely that for these complexes, the host spacer bridges adopt the most stable linker conformations (e.g., *gauche* for cryptophane-A).^{26,40} Additionally, the CH_4 data may be readily compared to that obtained with xenon as the guest. For example, the magnitude of ΔG° for the $\text{CH}_4@1$ complex ($-12.4 \text{ kJ}\cdot\text{mol}^{-1}$) is significantly smaller in magnitude than that measured for the $\text{Xe}@1$ complex ($-22.8 \text{ kJ}\cdot\text{mol}^{-1}$), in part reflecting the smaller volume of methane ($V_{\text{vdw}} = 28 \text{ \AA}^3$) compared to that of a xenon atom ($V_{\text{vdw}} = 42 \text{ \AA}^3$). Indeed, since the cavity of **1** seems nearly optimized for xenon encapsulation (see below),^{5,34} it is likely that a cryptophane with an even smaller inner cavity would be suitable to maximize interactions with methane; the creation of such a new cryptophane would require further shortening of the length of the bridges connecting the two cyclotribenzylene units. Along these same lines, the $\text{CH}_4@1$ and $\text{CH}_4@2$ complexes both exhibit positive ΔS° , indicating that the order of the system decreases upon complexation. Besides the relatively low entropic price of conformational restriction that is likely paid upon formation of these complexes (and the high symmetry of the guest, likely reducing any effects of orientational entropy), the net positive entropies for complexation likely results from the relatively low van der Waals occupancy factor (i.e., CH_4 is much smaller than the cavity of both hosts, so the loose fit would allow for CH_4 to have more motional freedom within the cage than it does in the bulk solvent).

The energy barrier for dissociation ($\Delta G^\ddagger = 49.7 \text{ kJ mol}^{-1}$) was calculated from the Eyring plot in Figure 2a, comprising enthalpy and entropy barriers for dissociation of $\Delta H^\ddagger = 41.1 \text{ kJ mol}^{-1}$ and $\Delta S^\ddagger = -29 \text{ J mol}^{-1} \text{ K}^{-1}$, respectively, for the high- T fit. The large negative ΔS^\ddagger value suggests a strong reorganization of the portal of **1** to expel a methane molecule,⁴¹ likely indicating that the complex in the transition state has a strained, significantly more-rigid structure than the free species in the ground (i.e., decomplexed) state during the entering and exiting of the guest. However, this ΔS^\ddagger value for $\text{CH}_4@1$ binding is significantly different from that found for xenon complexation by the same host ($\Delta S^\ddagger = -74 \text{ J mol}^{-1} \text{ K}^{-1}$),³⁴ consistent with a reduction of the entropy barrier of dissociation associated with a decrease of the size of the guest molecule that must pass through the portals of a given host. Indeed, it is also apparent when comparing $\text{Xe}@$ cryptophane activation entropies, the larger negative ΔS^\ddagger value for $\text{Xe}@1$ vs $\text{Xe}@2$ indicates that **1** must undergo more conformational strain (and hence limitation of motional freedom) to release xenon from the cavity than **2**, as **1** has much smaller portals for the guest to escape (such differences become even clearer when examining the so-called constrictive binding energy—see below). Naturally, the strain

on the cage portals has enthalpic consequences as well; for example, when comparing the activation enthalpies for xenon encapsulation by **1** and **2**, the ΔH^\ddagger value for $\text{Xe}@1$ is $\sim 8 \text{ kJ}\cdot\text{mol}^{-1}$ higher than that of $\text{Xe}@2$, consistent with the smaller cage having to adopt more unfavorable configurations in order to allow passage of a relatively large Xe atom. Qualitatively similar results would likely be found for methane complexation when comparing the two cages, given that ΔG^\ddagger is about 6 kJ mol^{-1} larger for $\text{CH}_4@1$ than $\text{CH}_4@2$ (about half the difference in the corresponding numbers for xenon, consistent with expectations based on methane's smaller size and roughly similar geometry compared to xenon). In any case, the values of E_a and ΔH^\ddagger are still relatively low for these complexes, giving rise to overall fast rates of decomplexation when compared to other host–guest systems (particularly those with ionic guests).⁴²

The data collected for the $\text{CH}_4@1$ complex confirms that **1** is an efficient host molecule for encapsulating methane in solution. Previously, it was reported by Boulard et al. that cryptophane-A (**2**) could be used as methane sensor in water when embedded in a polymer matrix.⁴³ According to the data reported in this article, significantly improved results should be expected with a host based on the structure of **1** because of its higher affinity for methane. However, the presence of methanedioxy linkers would largely prevent the use of **1** for such applications, and a corresponding change in the nature of the bridges would be needed to provide more robust molecular hosts (that would also be soluble in water). Synthetically speaking, we note that the replacement of the six oxygen atoms by six carbon atoms could be an interesting approach, as it would provide a much more thermally and chemically stable host molecule without significantly changing the size of the internal cavity.

Complexation of Other Small Gases by 1. The results concerning the complexation of methane by **1** prompted the investigation of other small gases as potential guests for this host; correspondingly, studies of the interactions between **1** and chloromethane, dichloromethane, carbon dioxide, ethane, propane, and ethylene gas molecules are reported here, along with our preliminary studies of molecular hydrogen complexation. These molecules have also been chosen because, like methane and xenon, in principle they have molecular volumes small enough to occupy the cavity of **1** (see Chart 2). However, in addition to their range of sizes these molecules possess different symmetries that might influence their binding properties with **1**; chloromethane, dichloromethane, hydrogen, carbon dioxide, ethane, propane, and ethylene belong respectively to the C_{3v} , C_{2v} , $D_{\infty h}$, $D_{\infty h}$, D_{3d} , C_{2v} , and D_{2h} point groups. In addition, except for CO_2 , all of these gasses possess protons that facilitate the detection of the complex by guest ^1H NMR spectroscopy. Among all of the molecules of the series, only CO_2 , H_2 , ethane, and ethylene were able to enter the cavity of **1** according to the observations of the host and guest NMR resonances. For example, despite the absence of proton spins, the successful binding of CO_2 to **1** may be inferred from the appearance of characteristic splittings of the *host* aromatic resonances upon guest binding (not shown; see for example ref 34).

In contrast to other ligands presently studied, H_2 complexation is manifested spectrally by fast exchange throughout virtually the entire range of available conditions;⁴⁴ significant broadening of the guest resonance (toward conditions of intermediate exchange) is observed only at the lowest temperatures (Figure 4(a)). As shown in the figure, the H_2 resonance in the presence of **1** shifts strongly upfield as the temperature is reduced. However, in the absence of host, there is virtually no shift of

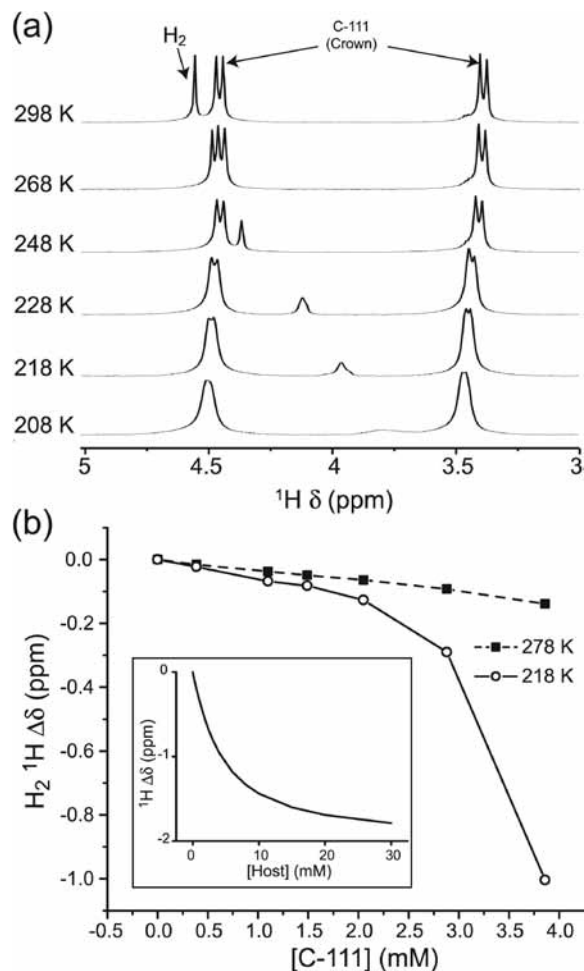


Figure 4. (a) Relevant portions of selected ^1H VT NMR spectra showing the strong temperature-dependent shift and broadening of the H_2 guest resonance in the presence of C-111 host (**1**) ($\sim 4 \text{ mM}$). (b) Dependence of the observed H_2 chemical shift (referenced to that in pure solvent) as a function of C-111 (**1**) concentration at two different temperatures: 278 K (filled squares/dashed lines) and 218 K (open circles/solid lines). Lines are meant only to guide the eye. Inset: calculated curve simulating the expected behavior of the guest chemical shift as a function of host concentration assuming a simple one-site (1:1) binding model under fast exchange condition (here, arbitrarily using values of $K = 300 \text{ M}^{-1}$ and limiting shift $\Delta\delta = (-)2 \text{ ppm}$).

the H_2 resonance in the bulk solvent as temperature is varied (see for example, the first points in Figure 4(b)), confirming the formation of a complex between H_2 and **1**. While a number of complexes and materials have been shown to bind molecular hydrogen (often under high pressure),^{45–53} to our knowledge **1** is the first organic cage shown to reversibly trap H_2 under near-ambient solution conditions. Upon closer inspection of these preliminary results, the H_2 ^1H chemical shift exhibits a complex dependence on temperature and host concentration that cannot be qualitatively reproduced by a simple 1:1 host–guest binding model (see for example, refs 54, 55). In such a case, the observed differential shift should asymptotically approach the limiting chemical shift (i.e., the chemical shift in the limit of infinite host concentration) as the host concentration increases (Figure 4(b) inset); however, at higher concentrations of **1** (and lower temperatures), the H_2 chemical shift dependence clearly diverges with increasing host concentration (e.g., Figure 4(b)). A full reporting of our studies of **1**– H_2 complexation, along with our ongoing efforts to model and characterize the nature of the binding in this system will be reported later in greater detail in part 2 of this contribution.³⁵

No evidence of binding from host or guest resonances was observed for chloromethane, dichloromethane, and propane. Indeed, such absence of spectral changes upon administration of these gases—even at the lowest temperatures studied—suggests that these molecules were too “large” (or sterically hindered) to enter the cavity of **1**. The chloromethane molecule is a particularly interesting case to discuss even though it is not recognized by **1** (see Supporting Information). Chloromethane possesses essentially the same molecular volume as a xenon atom (42 \AA^3), the latter being capable of binding to **1** with an exceptionally strong affinity ($K_a = 10^4 \text{ M}^{-1}$ at 298 K).³⁴ Participation in such host–guest binding is normally considered to be primarily determined by occupancy factor (i.e., the relative van der Waals volumes of the host cavity and the prospective guest), with $\sim 55\%$ being considered as the optimal occupancy factor in the absence of strong intermolecular forces.⁵⁶ Given this fact, it is intriguing to consider why two different guest molecules possessing similar volumes exhibit such different behavior with the same molecular host. Considering the structural features of these two species, the strong selectivity observed for binding xenon vs chloromethane is likely the result of some combination of differences in molecular geometry and/or electronic properties. First, whereas the Xe atom is obviously spherical, chloromethane has an almost cylindrical overall shape, which may be less ideal for the constrained geometry of the cavity of **1**. Alternatively, because of chloromethane’s composition and geometry, it possesses a permanent dipole moment, which also contributes to a higher polarizability; the familiar polarizability term refers to the distortion of the electronic cloud by an electric field, and the presence of a dipole moment in the chloromethane molecule ($\mu = 1.87 \text{ D}$) makes the chloromethane molecule more polarizable ($P = 4.7 \text{ \AA}^3$) than a xenon atom ($P = 4.04 \text{ \AA}^3$); even the polarizability of C_2H_4 is higher than Xe at 4.19 \AA^3 .⁵⁷ However, we note that the classical definition of “polarizability” does not seem to be the appropriate parameter to differentiate such guest molecules since this term invites a direct comparison between guest molecules having very different properties (e.g., atoms vs molecules, and those with and without permanent dipole moments). Reisse and co-workers previously pointed out this problem and have suggested that a clear distinction should be made between molecular polarity and molecular polarization due to the contribution of higher electric moments (quadrupole, octupole, ...) that can exist even for molecules with no apparent dipole moment.⁵⁸ The xenon atom has no dipole moment but is composed of a single nucleus surrounded by an electronic cloud that can easily distort under the influence of an electric field; possession of a more easily deformable electronic cloud should enable more facile entry across the portals of **1** and subsequent binding. Conversely, the chloromethane molecule, thus constituted by several atoms with relatively low individual polarizabilities (respectively 0.766, 1.76, and 2.18 \AA^3 for H, C, and Cl) possesses a rigid skeleton and electronic distribution less favorable to distortion (even though the chloromethane molecule has a higher apparent polarizability). Thus, using a familiar terminology, we can refer to the xenon atom as a “soft sphere” in contrast to the constituents of the chloromethane molecule (“hard sphere”) to reflect this fact. In any case, further computational efforts could shed additional light on the origins of the differences in binding of Xe and chloromethane by **1** (but such efforts are outside the scope of the current work).

The apparent failure of dichloromethane and propane to associate with **1** is likely the result of the relatively large size of these molecules, which could simply prevent them from being

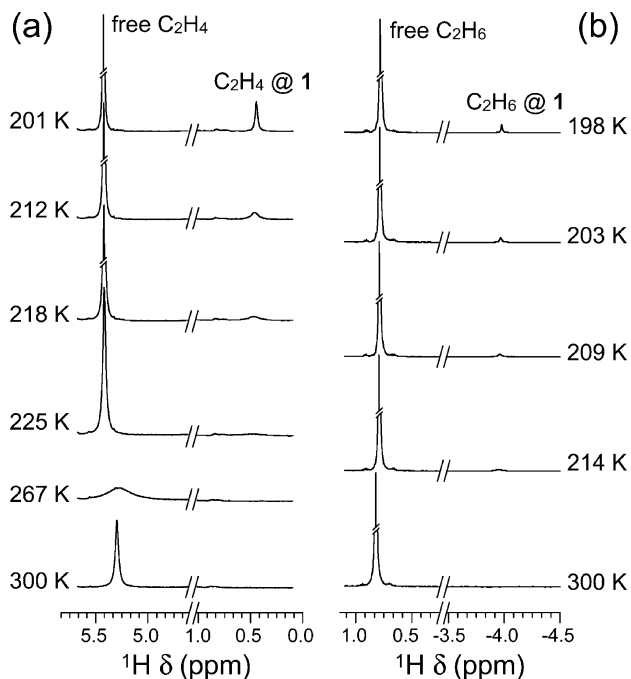


Figure 5. Relevant portions of selected ^1H VT NMR spectra respectively showing the formation of (a) the $\text{C}_2\text{H}_4@1$ complex and (b) the $\text{C}_2\text{H}_6@1$ complex.

accommodated inside the host's cavity. For instance, the dichloromethane molecule has a larger volume ($V_{\text{vdw}} = 56 \text{ \AA}^3$) than chloromethane ($V_{\text{vdw}} = 42 \text{ \AA}^3$) and a more extended geometry, thus the absence of complexation with CH_2Cl_2 is not surprising. Even though CH_2Cl_2 is technically small enough to be accommodated within the cavity of **1** (81 \AA^3), it is probably too large to cross the portals of this cryptophane, whose size has been estimated to be $\sim 9 \text{ \AA}^2$ ($\sim 2.3 \text{ \AA} \times \sim 3.8 \text{ \AA}$) for the empty host from MM3 molecular modeling (data given for distances between aromatic hydrogen atoms; see Supporting Information in ref 34). Propane, which has a larger molecular volume than dichloromethane ($V_{\text{vdw}} = 62 \text{ \AA}^3$), would give rise to a complex with **1** with an occupancy factor $\rho = 0.77$ (the guest/host molecular volumes ratio), likely too large to easily enter and remain within the cavity of **1**.⁵⁶ In addition, such complexation of **1** should be strongly entropically disfavored, as the complexation of the propane molecule would lead to a highly strained complex with greatly reduced conformational freedom.

In the light of the above results, we also investigated the binding of ethane and ethylene by **1** under the same experimental conditions. These two molecules possess molecular volumes similar to that of a xenon atom (40 and 45 \AA^3 for ethylene and ethane molecules, respectively), potentially allowing them to enter the cavity of **1**. Indeed, complexation of ethane and ethylene is manifested by the appearance of a new upfield-shifted peak in the ^1H NMR spectra at sufficiently reduced temperatures (Figure 5). While broad and weak, such peaks are clearly observed at $\sim 0.45 \text{ ppm}$ ($\Delta\delta = 5.0 \text{ ppm}$ between the free and bound guest resonances) and $\sim -4.0 \text{ ppm}$ ($\Delta\delta = 4.8 \text{ ppm}$) for the $\text{C}_2\text{H}_4@1$ and the $\text{C}_2\text{H}_6@1$ complexes, respectively.

Observation of C_2H_4 and C_2H_6 binding in the slow-exchange regime allows ready extraction of thermodynamic and kinetic data from Eyring, Arrhenius, and van't Hoff plots (Figure 6). The data were well-reproduced by linear fits, giving values summarized in Table 1. As with methane complexation, encapsulation of these two guests yields high-field shifted signals

due to the shielding effect of the host's six aromatic units; however, the complexation of ethane and ethylene appears much less efficient, as evidenced by the thermodynamical data extracted from the van't Hoff plots (Figure 6, parts (c) and (f)). For example, an extrapolated binding constant $K_a = 2.4 \text{ M}^{-1}$ at 298 K was calculated for the $\text{C}_2\text{H}_6@1$ complex; a slightly higher value ($K_a = 22.5 \text{ M}^{-1}$ at 298 K) was calculated for the $\text{C}_2\text{H}_4@1$ complex. These two K_a values are significantly smaller than that of the $\text{CH}_4@1$ complex, thus indicating that **1** is a highly selective host for the complexation of small hydrocarbons. In contrast to what is observed with methane, the formation of the $\text{C}_2\text{H}_6@1$ and $\text{C}_2\text{H}_4@1$ complexes appears enthalpically driven ($\Delta H^\circ = -9.3$ and -6.5 kJ mol^{-1} , respectively) but entropically disfavored ($\Delta S^\circ = -14.7$ and $-5.4 \text{ J mol}^{-1} \text{ K}^{-1}$, respectively). The negative entropy values indicate an increase in order upon complexation for these systems that is likely a consequence of the restricted motion of the two guests inside the cavity of host **1**. For example, according to the calculated structure of $\text{C}_2\text{H}_4@1$ (Figure 7), the plane of the ethylene molecule bound within **1** lies at a skewed (i.e., less than perpendicular) angle relative to the cage's C_3 axis; this nonideal configuration may be compared with the case of chloroform binding in **2** and cryptophane-E, where the C_3 axis of this squat C_{3v} guest is lined up with that of host.^{59,60} In any case, this assumption is consistent with the fact that an even larger negative ΔS° value was found for ethane than for ethylene (the latter being a smaller, planar molecule with greater internal rigidity).

The energy barriers for dissociation have also been calculated for these two guest molecules from the Eyring plots (Figure 6, parts (a) and (d)), and show similar values for ΔG^\ddagger (46.4 and 45.4 kJ mol^{-1} for ethane and ethylene, respectively) with correspondingly similar enthalpy barriers for dissociation ($\Delta H^\ddagger = 36.9$ and 36.4 kJ mol^{-1} , respectively) and calculated entropy barriers for dissociation ($\Delta S^\ddagger = -31.8$ and $-30.8 \text{ J mol}^{-1} \text{ K}^{-1}$, respectively). At first glance, it may be surprising that the ΔG^\ddagger values (and corresponding ΔH^\ddagger values) for $\text{C}_2\text{H}_4@1$ and $\text{C}_2\text{H}_6@1$ are smaller than those for $\text{CH}_4@1$; however, it is likely that these discrepancies primarily reflect the far greater stabilization of the $\text{CH}_4@1$ complex rather than a relative destabilization of the transition state for CH_4 binding.

Considerations of Constrictive Binding Energy. To remove the contribution from complex stabilization and to quantify the difficulty for a host to expel a given guest, it is useful to calculate the constrictive binding energy, defined by $\Delta G_{\text{const}}^\ddagger = \Delta G^\ddagger - (-\Delta G^\circ)$ (Figure 8). Constrictive binding energy includes the steric interactions that must be overcome for guest ejection and is a concept commonly applied to describe ligand binding interactions with respect to variable host aperture size.⁴² According to the literature,⁴² the trend of increasing $\Delta G_{\text{const}}^\ddagger$ should be based simply on the size of the guest; however, as described above, when CH_3Cl ($V_{\text{vdw}} = 42 \text{ \AA}^3$) was introduced to a solution of cryptophane-111 (**1**), no binding was observed even though it is essentially the same size as xenon and smaller than C_2H_6 (both of which do bind within the cryptophane-111 (**1**) cavity). However, direct quantitative comparison can be made between the complexes $\text{Xe}@1$ and $\text{Xe}@2$, and $\text{CH}_4@1$ and $\text{CH}_4@2$. As reported in Table 2, the constrictive binding energy of $\text{Xe}@1$ is $\sim 8 \text{ kJ mol}^{-1}$ higher than that of $\text{Xe}@2$, indicating a more difficult accessibility of the guest for host **1** than for cryptophane-A (**2**). Similarly, the $\Delta G_{\text{const}}^\ddagger$ values for $\text{CH}_4@1$ is nearly 5 kJ mol^{-1} higher than that of $\text{CH}_4@2$.

To compare the complexation of the hydrocarbon gases by **1** at room temperature, the constrictive binding energies ($\Delta G_{\text{const}}^\ddagger$)

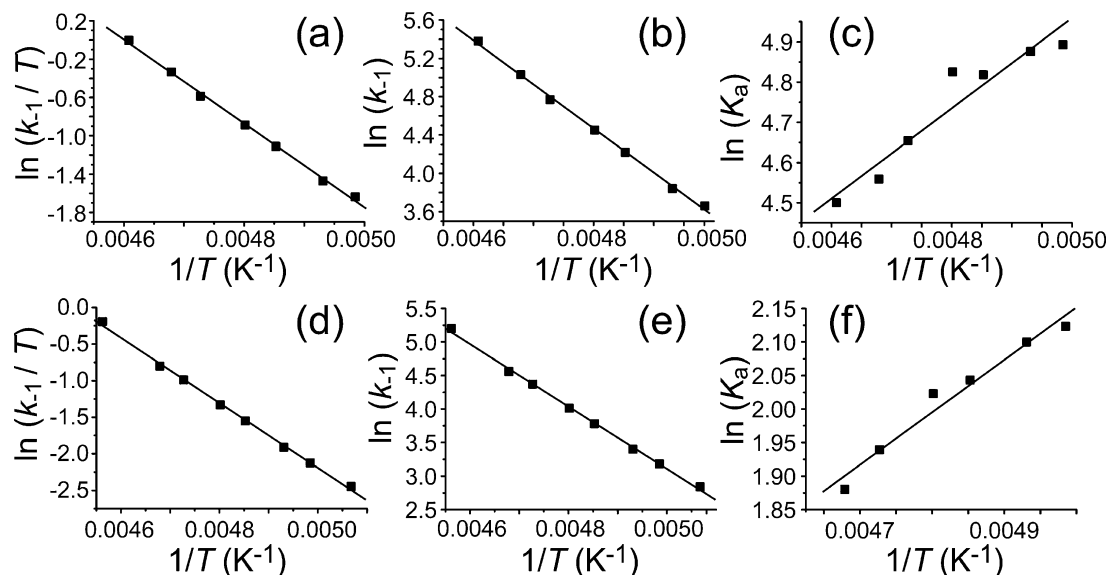


Figure 6. Eyring, Arrhenius, and van't Hoff plots for the determination of kinetic and thermodynamic data. (a–c) Ethylene; (d–f) ethane.

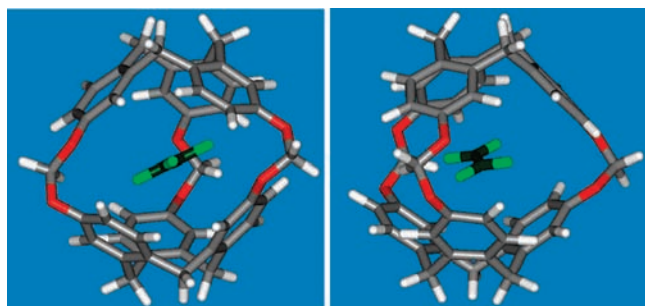


Figure 7. Two views of the calculated “stick” structure for the complex of cryptophane-111 host (**1**) and ethylene guest (highlighted in green).

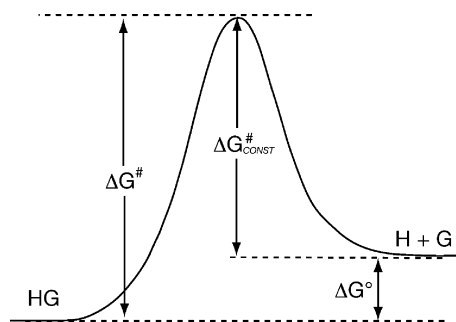


Figure 8. Constrictive binding energy coordinate diagram for host–guest decomplexation (after ref 42). Constrictive binding via encapsulation results in complexes with relatively high kinetic stabilities.

for methane, ethylene, and ethane guest molecules are calculated to be 38.0, 37.7, and 44.1 kJ mol⁻¹, respectively. These results indicate that more free energy is needed at the transition state to enable an ethane molecule to transit a portal of **1** than an ethylene or a methane molecule. Not only is portal configuration important when considering enthalpic and entropic contributions to $\Delta G^{\ddagger}_{CONST}$, but also ligand reorganization/rearrangement can also play a role (i.e., in order for binding or expulsion of a guest to occur, the ligand and the host must be arranged in such a way, with respect to one another—and with respect to the internal configuration of a flexible guest—to allow the guest to enter or exit the cavity); correspondingly, such effects may also be contributing to the larger $\Delta G^{\ddagger}_{CONST}$ for ethane. In contrast, even though methane is smaller than ethylene, their constrictive

TABLE 2: Constrictive Binding Energies of Selected Cryptophane Complexes at Room Temperature

guest	V_{vdw} (Å ³)	host	$\Delta G^{\ddagger}_{CONST}$ (kJ mol ⁻¹)	$\Delta H^{\ddagger}_{CONST}$ (kJ mol ⁻¹)	$\Delta S^{\ddagger}_{CONST}$ (J mol ⁻¹ K ⁻¹)
Xe ³⁴	42	1	42.1		
CH ₄	28	1	38.0	31.2	-22.7
C ₂ H ₄	40	1	37.7	27.1	-36.2
C ₂ H ₆	45	1	44.1	30.3	-46.5
Xe ^{29,65}	42	2	34.3		
CH ₄ ^{16,33}	28	2	32.7		

binding energies are essentially the same (within error). Although such independence of $\Delta G^{\ddagger}_{CONST}$ has been observed for the association of different guests by larger hosts (e.g., Cram's hemicarcerands),⁶¹ with much greater portal flexibility than **1**, these results do not support the expectation that constrictive binding should be based on guest size with no account of other potential contributions (e.g., the relative geometries of the host portals and a given guest).^{42,62} For example, the relatively low value for $\Delta G^{\ddagger}_{CONST}$ for C₂H₄ with respect to the other hydrocarbons, and Xe, may reflect its flat geometry, which in turn may require less portal reorganization for accommodation by **1**. Knowledge of ΔS^{\ddagger} , ΔS° , ΔH^{\ddagger} , and ΔH° allows ready calculation of $\Delta S^{\ddagger}_{CONST}$ and $\Delta H^{\ddagger}_{CONST}$, and thus a closer look at the relative enthalpic and entropic contributions that give rise to the above $\Delta G^{\ddagger}_{CONST}$ values (Table 2). For example, large differences (>10 J mol⁻¹·K⁻¹) in the magnitudes of $\Delta S^{\ddagger}_{CONST}$ for the three complexes are observed, with the results following the expected trend (i.e., with the constrictive binding of the largest of the three guests, C₂H₆, being the most entropically unfavorable); yet it should be noted that the sizes of these differences are likely exacerbated by contributions from orientational entropy and the reduction of internal freedom of the guest (contributions that for these three molecules, would be expected to follow the same trend as the overall size). In contrast, $\Delta H^{\ddagger}_{CONST}$ values for the three complexes are surprisingly similar, with C₂H₄ actually having the smallest value by a small amount, perhaps indeed reflecting the reduced energetic price that must be paid to allow passage of the flat ethylene molecule, as suggested above.

5. Conclusions

We have studied the solution-phase interactions between the recently synthesized cryptophane-111 (**1**) and a series of small

potential guest molecules, including the simple hydrocarbons methane, ethane, and ethylene. The binding of these molecules by **1** has been studied by ^1H NMR spectroscopy, allowing kinetic and thermodynamic data to be extracted for the resulting complexes. It was shown that cryptophane-111 (**1**) exhibits a relatively good affinity for CH_4 , with a binding constant of 148 M^{-1} at 298 K, making **1** a better molecular host than cryptophane-A (**2**) for encapsulating CH_4 in organic solution. In addition, Host **1** presents a K_a value of similar magnitude toward CH_4 compared to other synthetic molecular hosts previously reported in the literature. For instance, Rebek and co-workers,¹⁹ and Nakazawa et al.,³⁰ have reported molecular hosts with K_a values for CH_4 at room temperature of 300 M^{-1} and 81 M^{-1} respectively, and weaker, but rather comparable, K_a values for C_2H_4 of 280 M^{-1} and 49 M^{-1} , respectively. Here, the selectivity of **1** is well-demonstrated by its preference for the smallest hydrocarbons, as ethylene and ethane are recognized with much smaller association constants ($K_a = 22 \text{ M}^{-1}$ and 2 M^{-1} , respectively) than that of methane, and propane binding within the cavity of **1** was not observed. Thus, given that cryptophane-A (**2**) has already been demonstrated as a sensor for methane dissolved in water, arguably a more potent sensor should be obtained if the structure of **1** could be altered to improve its stability and aqueous solubility while maintaining the properties of its cavity.

Interestingly, it was demonstrated that **1** does not exhibit any affinity for chloromethane, even though it possesses the same volume as a xenon atom, the latter possessing a remarkably strong binding constant of 10^4 M^{-1} under similar experimental conditions. The difference in behavior observed for these two guests toward **1** was rationalized in terms of the differences in the geometries and electronic properties between these two similarly sized species, and demonstrates the importance of other considerations beyond overall size when designing novel host molecules for next-generation applications. Separately, molecular hydrogen (H_2) gas was also observed to bind **1**, but the complexation was manifested in the spectra by fast exchange throughout the entire range of available conditions, in contrast to the other ligands studied here; moreover, an unexpected ^1H chemical shift dependence upon temperature and host concentration was observed for the guest resonance that is not consistent with a 1:1 host:guest ratio (results to be reported in greater detail in part 2 of this contribution).³⁵ Taken together, these results prompt the development of new small congeners of **1** aimed at increasing both the host stability and its selectivity toward a given guest. Finally, the investigation of complexation of other small neutral species by **1** (e.g., other noble gases, CO_x , NO_x , etc.), as well as liquid-crystal NMR studies of such cryptophane host–guest interactions,^{63,64} are ongoing and will be reported in due course.

Acknowledgment. J.-P.D. and T.B. would like to thank the National Research Agency (ANR program “Physico-Chimie du Vivant 2006”) and the “Cluster Recherche Chimie, Région Rhône-Alpes” for financial support. K.E.C. gratefully acknowledges the Fulbright Scholar Program and H.A.F. acknowledges an NSF IRFP fellowship grant (Grant No. 0502393). B.M.G. thanks Qingfeng Ge and Lichang Wang for helpful conversations; B.M.G. is a Cottrell Scholar of Research Corp. B.M.G. and K.E.C. are supported in part by NSF CHE-0349255.

Supporting Information Available: Figure S1 demonstrating the lack of CH_3Cl binding by **1** (VT ^1H NMR spectra). This material is available free of charge via the Internet at <http://pubs.acs.org>.

References and Notes

- (1) Cram, D. J.; Cram, J. M. *Container Molecules and Their Guests*; Royal Soc. Chem.: Cambridge, UK, 1994; Vol. 4.
- (2) Rudkevich, D. M. *Bull. Chem. Soc. Jpn.* **2002**, *75*, 393.
- (3) Rudkevich, D. M. *Angew. Chem., Int. Ed.* **2004**, *43*, 558.
- (4) Warmuth, R.; Yoon, J. *Acc. Chem. Res.* **2001**, *34*, 95.
- (5) Rebek, J. J. *Angew. Chem., Int. Ed.* **2005**, *44*, 2068.
- (6) Schmuck, C. *Angew. Chem., Int. Ed.* **2007**, *46*, 5830.
- (7) Schramm, M. P.; Restorp, P.; Zelder, F.; Rebek, J. *J. Am. Chem. Soc.* **2008**, *130*, 2450.
- (8) Liu, S.; Gibb, B. C. *Chem. Comm.* **2008**, 3709.
- (9) Kawano, M.; Kobayashi, Y.; Ozeki, T.; Fujita, M. *J. Am. Chem. Soc.* **2006**, *128*, 6558.
- (10) Fielder, D.; Bergman, R. B.; Raymond, K. N. *Angew. Chem., Int. Ed.* **2006**, *45*, 745.
- (11) Kaanumalle, L. S.; Ramamurthy, V. *Chem. Comm.* **2007**, 1062.
- (12) Fakayode, S. O.; Lowery, M.; Fletcher, K. A.; Huang, X.; Powe, A. M.; Warner, I. M. *Curr. Anal. Chem.* **2007**, *3*, 171.
- (13) *Nanoporous Materials*; Nangia, A., Ed.; Imperial College Press: London, 2004; Vol. 4, p 165.
- (14) Spence, M. M.; Ruiz, E. J.; Rubin, S. M.; Lowery, T. J.; Winsinger, N.; Schultz, P. G.; Wemmer, D. E.; Pines, A. *J. Am. Chem. Soc.* **2004**, *126*, 15287.
- (15) Kuhn, R.; Stoecklin, F. *Erni Chromatogr.* **1992**, *33*, 32.
- (16) Garel, L.; Dutasta, J.-P.; Collet, A. *Agnew. Chem. Int. Ed.* **1993**, *32*, 1169.
- (17) Fenyvesi, E.; Szente, L.; Russel, N. R.; McNamara, M. *Compr. Supramol. Chem.* **1996**, *3*, 305.
- (18) Cram, D. J.; Tanner, M. E.; Knobler, C. B. *J. Am. Chem. Soc.* **1991**, *113*, 7717.
- (19) Branda, N.; Wyler, R.; Rebek, J. *Science* **1994**, *363*, 1222.
- (20) Branda, N.; Grotzfeld, R. M.; Valdes, C.; Rebek, J. *J. Am. Chem. Soc.* **1995**, *117*, 85.
- (21) Canceill, J.; Lacombe, L.; Collet, A. *J. Am. Chem. Soc.* **1985**, *107*, 6993.
- (22) Canceill, J.; Lacombe, L.; Collet, A. *J. Am. Chem. Soc.* **1986**, *108*, 4230.
- (23) Canceill, J.; Cesario, M.; Collet, A.; Guilhem, J.; Riche, C.; Pascard, C. *J. Am. Chem. Soc. Chem. Comm.* **1986**, 339.
- (24) Canceill, J.; Lacombe, L.; Collet, A. *J. Chem. Soc., Chem. Commun.* **1987**, 219.
- (25) Brotin, T.; Dutasta, J.-P. *Chem. Rev.* **2009**, *109*, 88.
- (26) Bartik, K.; Luhmer, M.; Dutasta, J.-P.; Collet, A.; Reisse, J. *J. Am. Chem. Soc.* **1998**, *120*, 784.
- (27) Brotin, T.; Lesage, A.; Emsley, L.; Collet, A. *J. Am. Chem. Soc.* **2000**, *122*, 1171.
- (28) Brotin, T.; Barbe, R.; Darzac, M.; Dutasta, J. P. *Chem.—Eur. J.* **2003**, *9*, 5784.
- (29) Brotin, T.; Dutasta, J.-P. *Eur. J. Org. Chem.* **2003**, 973.
- (30) Nakazawa, J.; Sakae, Y.; Aida, M.; Naruta, Y. *J. Org. Chem.* **2007**, *72*, 9448.
- (31) Scarso, A.; Pellizzaro, L.; De Lucchi, O.; Linden, A.; Fabris, F. *Angew. Chem., Int. Ed.* **2007**, *46*, 4972.
- (32) Atwood, J. L.; Barbour, L. J.; Jerga, A. *Science* **2002**, *296*, 2367.
- (33) Garel, L.; Lozach, B.; Dutasta, J.-P.; Collet, A. *J. Am. Chem. Soc.* **1993**, *115*, 11652.
- (34) Fogarty, H. A.; Berthault, P.; Brotin, T.; Huber, G.; Desvaux, H.; Dutasta, J. P. *J. Am. Chem. Soc.* **2007**, *129*, 10332.
- (35) Chaffee, K. E.; Fogarty, H. A.; Brotin, T.; Goodson, B. M.; Dutasta, J. P. manuscript in preparation.
- (36) Huber, G.; Beguin, L.; Desvaux, H.; Brotin, T.; Fogarty, H. A.; Dutasta, J. P.; Berthault, P. *J. Phys. Chem. A* **2008**, *112*, 11363.
- (37) Canceill, J.; Collet, A. *J. Chem. Soc. Chem. Comm.* **1988**, *9*, 582.
- (38) Brotin, T.; Roy, V.; Dutasta, J. P. *J. Org. Chem.* **2005**, *70*, 6187.
- (39) Goto, H.; Osawa, E. *J. Chem. Soc., Perkin Trans.* **1993**, *2*, 187.
- (40) Luhmer, M.; Goodson, B. M.; Song, Y.-Q.; Laws, D. D.; Kaiser, L.; Cyrier, M. C.; Pines, A. *J. Am. Chem. Soc.* **1999**, *121*, 3502.
- (41) Darzac, M.; Brotin, T.; Rousset-Arzel, L.; Bouchu, D.; Dutasta, J.-P. *New J. Chem.* **2004**, *28*, 502.
- (42) Pluth, M. D.; Raymond, K. N. *Chem. Soc. Rev.* **2006**, *36*, 161.
- (43) Boulard, C.; Mowlem, M. C.; Connelly, D. P.; Dutasta, J. P.; German, C. R. *Optics Express* **2008**, *16*, 12607.
- (44) Macomber, R. S. *J. Chem. Educ.* **1992**, *69*, 105.
- (45) Millar, J. M.; Kastrup, R. V.; Melchior, M. T.; Horvath, I. T. *J. Am. Chem. Soc.* **1990**, *112*, 9643.
- (46) Yoon, J.-H.; Heo, N. H. *J. Phys. Chem.* **1992**, *96*, 4997.
- (47) Vigalok, A.; Ben-David, Y.; Milstein, D. *Organometallics* **1996**, *15*, 1839.
- (48) Krishnan, V. V.; Suib, S. K.; Corbin, D. R.; Schwarz, S.; Jones, G. L. *Chem. Comm.* **1996**, 395.
- (49) Weitkamp, J.; Ernst, S.; Cubero, F.; Wester, F.; Schnick, W. *Adv. Mater.* **1997**, *9*, 247.

- (50) Liu, C.; Fan, Y. Y.; Liu, M.; Cong, H. T.; Cheng, H. M.; Dresselhaus, M. S. *Science* **1999**, 286, 1127.
- (51) Zhao, Y.; Kim, Y. H.; Dillon, A. C.; Heben, M. J.; Zhang, S. B. *Phys. Rev. Lett.* **2005**, 94, 155504.
- (52) Neiner, D.; Okamoto, N. L.; Condron, C. L.; Ramasse, Q. M.; Yu, P.; Browning, N. D.; Kauzlarich, S. M. *J. Am. Chem. Soc.* **2007**, 129, 13857.
- (53) Murata, Y.; Maeda, S.; Murata, M.; Komatsu, K. *J. Am. Chem. Soc.* **2008**, 130, 6702.
- (54) Bartik, K.; Luhmer, M.; Heyes, S. J.; Ottinger, R.; Reisse, J. *J. Magn. Reson. B* **1995**, 109, 164.
- (55) Rubin, S. M.; Spence, M. M.; Goodson, B. M.; Wemmer, D. E.; Pines, A. *Proc. Natl. Acad. Sci. U.S.A.* **2000**, 97, 9472.
- (56) Mecozzi, S.; Rebek, J., Jr. *Chem. Eur. J.* **1998**, 4, 1016.
- (57) Schlitz, M. PhD thesis 1997. Universite de Paris Sud (France). No. 97 PA11 2010.
- (58) Bartik, K.; Luhmer, M.; Collet, A.; Reisse, J. *Chirality* **2001**, 13, 2.
- (59) Cavagnat, D.; Brotin, T.; Bruneel, J.-L.; Dutasta, J.-P.; Thozet, A.; Perrin, M.; Guillaume, F. *J. Phys. Chem. B* **2004**, 108, 5572.
- (60) Canceill, J.; Cesario, M.; Collet, A.; Guilhem, J.; Lacombe, L.; Lozach, B.; Pascard, C. *Angew. Chem., Int. Ed.* **1989**, 9, 1246.
- (61) Cram, D. J.; Blanda, M. T.; Paek, K.; Knobler, C. B. *J. Am. Chem. Soc.* **1992**, 114, 7765.
- (62) Steed, J. W.; Atwood, J. *Supramolecular Chemistry*, 2nd. ed.; Wiley: New York, 2009.
- (63) Marjanska, M.; Goodson, B. M.; Castiglione, F.; Pines, A. *J. Phys. Chem. B* **2003**, 107, 12558.
- (64) Chaffee, K. E.; Marjanska, M.; Goodson, B. M. *Solid State Nucl. Magn. Reson.* **2006**, 29, 104.
- (65) Brotin, T.; Devic, T.; Lesage, A.; Emsley, L.; Collet, A. *Chem. Eur. J.* **2001**, 7, 1561.

JP903452K